*Journal of Applied Mechanics and Technical Physics, Vol. 47, No. 5, pp. 671–678, 2006*

# TURBULENT FLOW PAST A TRANSVERSE CAVITY WITH INCLINED SIDE WALLS. 1. FLOW STRUCTURE

**A. Yu. D'yachenko, V. I. Terekhov, and N. I. Yarygina**

UDC 536.24

*The process of vortex formation in a cavity with inclined walls, which has a moderate aspect ratio, is experimentally studied, and the distribution of pressure coefficients is measured. The angle of inclination of the side walls $\varphi$ is varied from 30 to 90°. It is found that the flow in the cavity becomes unstable in the range of inclination angles $\varphi = 60$–70°. Flow reconstruction occurs, which substantially alters the surface-temperature and static-pressure distributions. Large changes in these characteristics and their nonuniform distributions for these angles are observed across the cavity on its frontal wall and on the bottom. For small angles ($\varphi = 30$ and 45°), the pressure on the rear wall drastically increases, which leads to a small increase in pressure averaged over the entire cavity surface.*

**Key words:** *turbulent flow, separated flow, boundary layer, cavity, vortex formation, pressure fields.*

**Introduction.** Cavities and notches are often encountered in heat-exchanger channels, in elements of flying vehicles and turbine facilities, and in many other devices. The problem of optimization of various methods of intensification or suppression of heat transfer in cavities and the search for effective removal of admixtures from notches are fairly urgent. The flow past a rectangular cavity was considered in numerous theoretical and experimental works dealing with investigating dynamic characteristics of the separated flow [1–12]. Thermal characteristics are less adequately studied, but their values are necessary for optimizing parameters of electric power plants and improving methods of numerical simulation of turbulent separated flows in cavities. There are only few publications that discuss three-dimensional effects of the flow in moderated-sized cavities, which are caused by the influence of the end faces of the channels (see, e.g., [1, 2, 6]). There are almost no studies of dynamic and thermal characteristics in cavities with inclined frontal and rear walls, which are promising from the viewpoint of heat-transfer intensification. Rare exceptions are some experimental activities [4, 13–15].

Let us consider the papers studying the three-dimensional structure of the vortex flow in a rectangular cavity aligned across the flow in more detail. It was found [6] that there are ordered three-dimensional structures of the type of the Taylor–Görtler vortices between the cavity walls and the primary vortex in the case of a laminar flow ahead of the cavity (Reynolds numbers $\mathrm{Re} < 10^4$) if the cavity aspect ratio is $S/L = 1$, 2, or 3. These vortices are destroyed as the Reynolds number reaches $\mathrm{Re} > 10^4$. Koseff and Street [7] who studied the behavior of the secondary vortex on the rear wall of the cavity with the geometry similar to that considered in [6] attributed this phenomenon to origination of turbulent fluctuations in the boundary layer, the energy of these fluctuations being higher than the energy of the laminar flow by more than an order of magnitude. Taylor–Görtler vortices are local three-dimensional structures caused by curvature of the streamlines of the separated flow.

Kutateladze Institute of Thermophysics, Siberian Division, Russian Academy of Sciences, Novosibirsk 630090; terekhov@itp.nsc.ru; yarygina@itp.nsc.ru. Translated from Prikladnaya Mekhanika i Tekhnicheskaya Fizika, Vol. 47, No. 5, pp. 68–76, September–October, 2006. Original article submitted August 25, 2005; revision submitted October 26, 2005.

0021-8944/06/4705-0671  

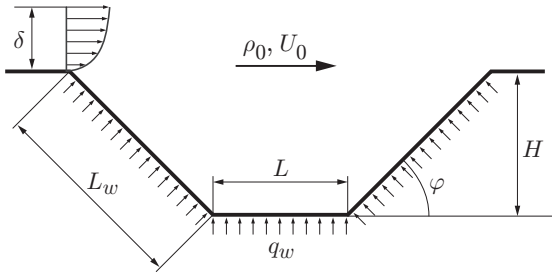


Fig. 1. Schematic of the cavity flow.

The specific features of the primary vortex in crossflow cavities with small aspect ratios include the cellular structure of the flow over the cavity span [1, 2, 8]. This manifestation of three-dimensionality significantly depends on the geometry of the rectangular cavity (on the ratio of the cavity width $L$ to its height $H$ and span $S$). It was shown in [1] for the first time that the primary vortex decomposes into cellular structures in cavities with low aspect ratios. The reason is the effect of shear gradients on the butt-end walls. These structures can be symmetric or asymmetric; as was found in [2], the flow structure depends on the cavity height, other conditions being identical. Based on an analysis of experimental results, Maull and East [1] concluded that three-dimensional cellular structures are observed in cavities with $0.4 < H/L < 0.9$, and the flow is two-dimensional in cavities with a square cross section. This conclusion is not obvious. It was shown [8] that the flow in a cavity with an aspect ratio $S/L = 2$, 4, 6, and 8 has a symmetric cellular structure; the number of cells is half the value of the aspect ratio. For $S/L = 3$, 5, and 7, the cellular structure is asymmetric. One of the edge cells is "incompletely" formed. Tornado-like motion at the interface between the primary vortex and the leading secondary vortex and mass ejection near the boundary between the cells are also noted in [8]. It follows from the model proposed in [2] and developed in [8] that the shear layer entering the cavity due to instability at the reattachment point transforms to tornado-like motion at the interface between two cells.

Three-dimensional effects on the pressure distribution and intensity of local heat transfer on the cavity bottom was studied only in [8] where spanwise measurements of a symmetric regular cellular structure were performed in a cavity with $S/L = 8$ and $H/L = 0.66$. The observed nonuniformity of the static-pressure and temperature fields was in line with the gas-dynamic structure of the flow. The structure of the three-dimensional flow and its dynamic and thermal characteristics in cavities with small aspect ratios aligned perpendicular to the flow have not been considered in detail until now.

In addition, separated flows in crossflow cavities with inclined walls have been weakly studied. According to [4], the inclination of the rear wall leads to attenuation of pressure fluctuations and the amplitude of hydrodynamic oscillations in the reattachment zone. Naturally, these effects are expected to influence flow instability and vortex formation.

**Test Technique and Analysis of Results.** The oil-film technique was used to visualize the flow pattern in crossflow cavities of moderate size ($S/L = 1$, 2, 3). We also considered cavities with a square cross section $60 \times 60$ mm and cavities with inclined walls (angles of inclination $\varphi = 90$, 80, 70, 60, 45, and 30°) (Fig. 1). In the experiments, the cavity was located at the bottom of a wind tunnel with the working-channel cross section $200 \times 200$ mm. The angle of inclination of the side walls was changed, whereas the cavity height $H$ and its length $L$ (in the streamwise direction) remained constant. Depending on the angle of inclination, the length of the side walls $L_w$ was also different. The experiments were performed in the range of Reynolds numbers based on the cavity height $\mathrm{Re}_H = 5 \cdot 10^4$–$3 \cdot 10^5$. The boundary layer ahead of the cavity was turbulent, and its thickness was 30–35 mm. It was believed for a long time that the cavity flow is always turbulent because the Kelvin–Helmholtz instability responsible for converting the flow in the shear layer to the turbulent state is developed near the separation point. In the circulation region, where the flow turns behind the reattachment point, however, the near-wall turbulent flow is laminarized under a favorable pressure gradient. The presence of a laminar–turbulent transition was established in [16, 17] on the basis of measuring the mean heat-transfer coefficients. In the present experiments, in a square cavity of size mentioned above, the transition corresponded to the value $\mathrm{Re}_H = 4.3 \cdot 10^4$ [18], i.e., the cavity flow was also turbulent in the above-given range of Reynolds numbers.

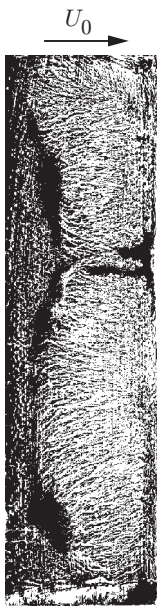


Fig. 2. Flow past a cavity with $\varphi = 90^\circ$ in the case of a two-cell structure [18].

Special attention was paid to ensure that the cavity was rigorously perpendicular to the flow because detailed studies showed that the flow in a rectangular cavity is unstable. A small deviation in the cavity alignment (within 1°) from the direction perpendicular to the flow violates the cavity-flow symmetry (Fig. 2). It is seen from Fig. 2 that a two-cell asymmetric structure of the primary vortex is formed at the bottom of a rectangular cavity.

If the cavity is rigorously perpendicular to the flow, the vortex-formation pattern in the cavity with $\varphi = 90^\circ$ is symmetric and contains one cell (Fig. 3). Figure 3 shows the unfolded picture of the visualized flow pattern on the bottom, side walls, and end face of the cavity for different values of the angle $\varphi$. These results were partly published in [13, 14, 19]. As the angle of inclination of the side walls is changed, the visualized patterns become essentially different. With the angle of inclination decreasing, flow three-dimensionality is seen more definitely. It is also seen that the primary vortex is located in the center of the cavity at $\varphi = 90^\circ$ and closer to the rear wall at $\varphi = 80^\circ$. In both cases, the primary vortex has the form of one cell. Further opening of the cavity enhances the asymmetry of shear stresses, which results in elliptic-type instability (terminology of [20]). At $\varphi < 70^\circ$, a powerful mass flux from the rear to the frontal wall arises in the center of the cavity, and the primary vortex decomposes into two cells. The two-cell structure persists at $\varphi = 30$, 45, and 60°. At $\varphi = 70^\circ$, the vortex-formation pattern is indistinct because of strong instability. In the case of the two-cell vortex structure, corner vortices start playing a more important role, and the primary vortex is displaced away from the walls. Nucleation of the crossflow mass flux on the rear wall and its impact onto the frontal wall are clearly visible. The vortex flow on the butt-end face of the cavity becomes asymmetric, and the center of the primary vortex is shifted toward the frontal wall. At $\varphi < 70^\circ$, the primary vortex decomposes into two vortices, which are displaced from the butt-end faces and become attached to the frontal wall.

The change in flow regimes from unstable one-cell to stable two-cell flow also depends on the Reynolds number (Fig. 4). The flow structure is most distinct at $\mathrm{Re}_H = 8 \cdot 10^4$. In was found in a cycle of experiments that vortex breakdown occurs at $\varphi \approx 60^\circ$ for $\mathrm{Re}_H = 4 \cdot 10^4$ and at $\varphi \approx 80^\circ$ for $\mathrm{Re}_H = 1.2 \cdot 10^5$. At $\varphi = 70^\circ$, the mass flux from the rear to the frontal wall is attenuated with increasing $\mathrm{Re}_H$.

The flow structure is in line with the temperature fields obtained by means of thermographic visualization with the use of an infrared imager (Fig. 5). In these experiments, the bottom was covered by an electroconducting graphite layer 40 $\mu$m thick, which served as a heater. Underneath the heater, there were Chromel–Copel thermocouples insulated from the heater by a layer of a heat-resistance varnish. The thermocouples were aligned over the cavity span with a gap of 10 mm and were used to "match" the thermal patterns in the infrared range obtained in experiments to real temperatures. Heating was performed in the regime with $q_w = \mathrm{const}$. Heat losses through the

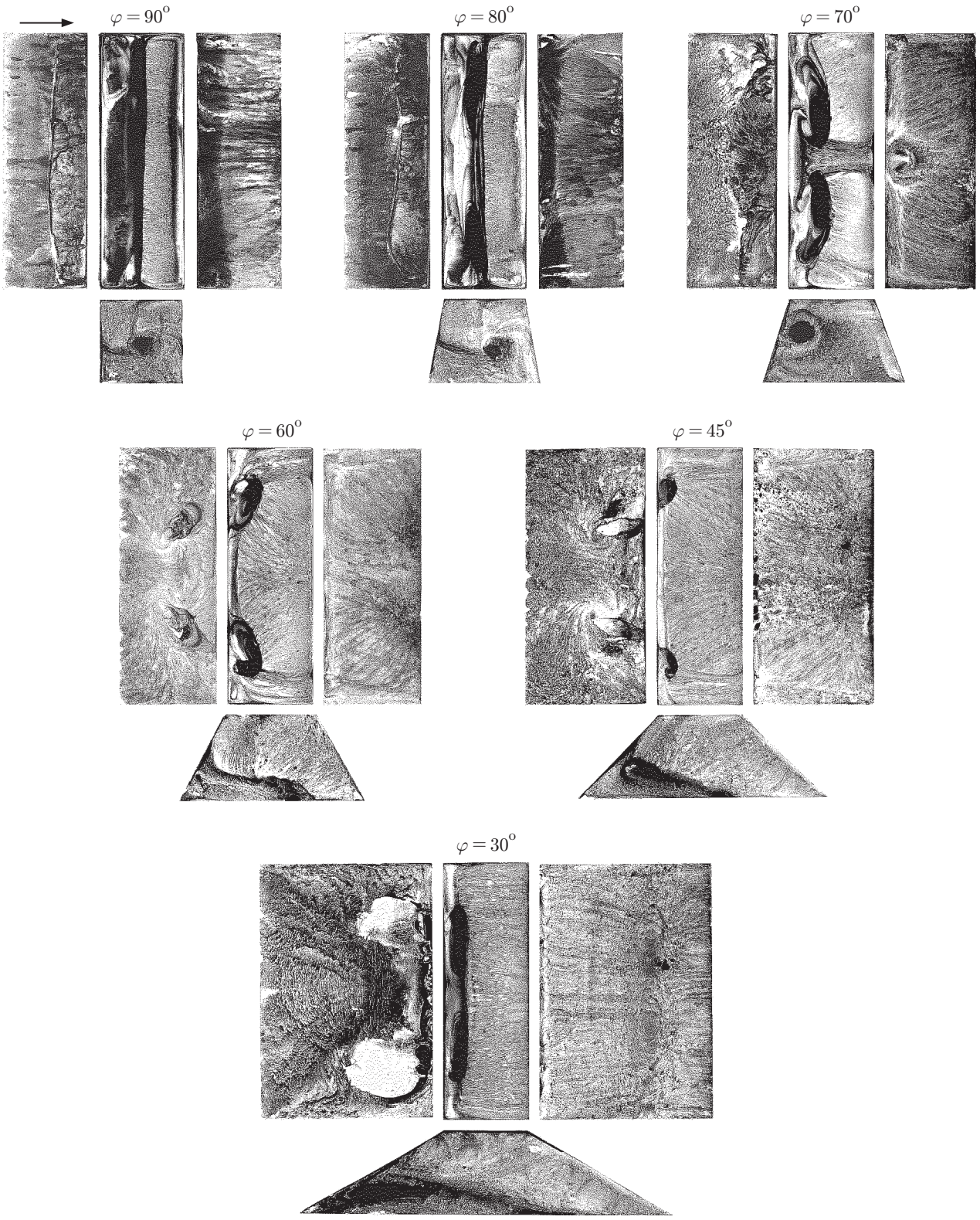


Fig. 3. Evolution of vortex formation in a cavity ($\mathrm{Re}_H = 8 \cdot 10^4$)

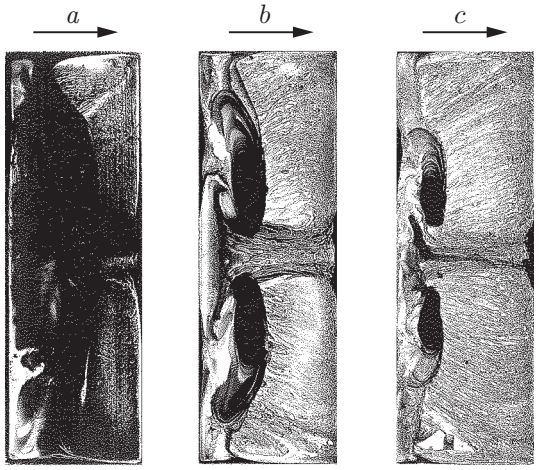


Fig. 4. Visualization of the flow on the cavity bottom for $\varphi = 70^\circ$: $\mathrm{Re}_H = 4 \cdot 10^4$ (a), $8 \cdot 10^4$ (b), and $1.2 \cdot 10^5$ (c).

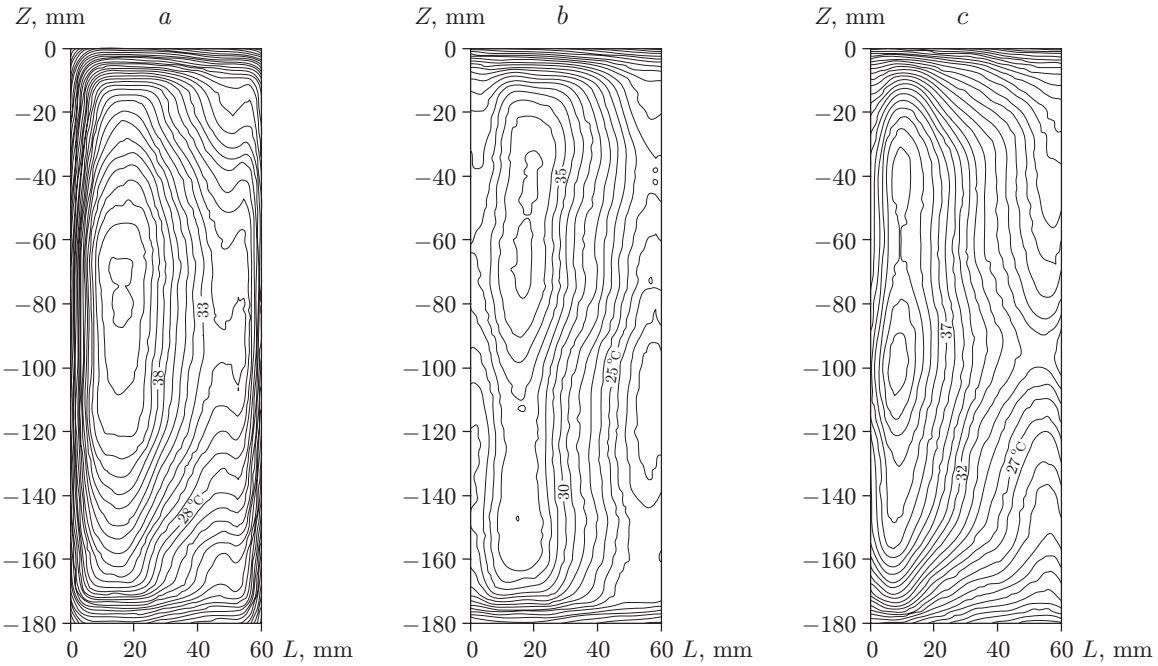


Fig. 5. Distribution of temperature on the cavity bottom for $\mathrm{Re}_H = 8 \cdot 10^4$: $\varphi = 90^\circ$ (a), $80^\circ$ (b), and $70^\circ$ (c).

bottom were estimated by the difference in temperature at the bottom plate and several thermocouples established on the lower surface. During thermographic visualization, the working section with the cavity was located vertically on the side wall of the wind-tunnel duct. The isotherms in Fig. 5 were determined by the difference in temperature on the wall and in the main flow. The isotherms obtained allow us to conclude that a vortex flow with a two-cell structure is formed in the vicinity of the rear wall in an inclined cavity with $\varphi = 70^\circ$. The temperature fields "reflect" the three-dimensional character of vortex formation near the cavity bottom and even flow asymmetry. The minimum temperature corresponds to the centers of large-scale vortex cells localized near the rear wall of the cavity.

The vortex pattern obtained correlates with the distribution of the pressure coefficient $C_p = 2(p_i - p_0)/(\rho U^2)$ on the bottom and walls of the cavity ($p_i$ is the pressure on the wall; $p_0$ and $U$ are the pressure and velocity measured at a height of 100 mm from the model surface ahead of the cavity). For all examined angles of the cavity, the pressure

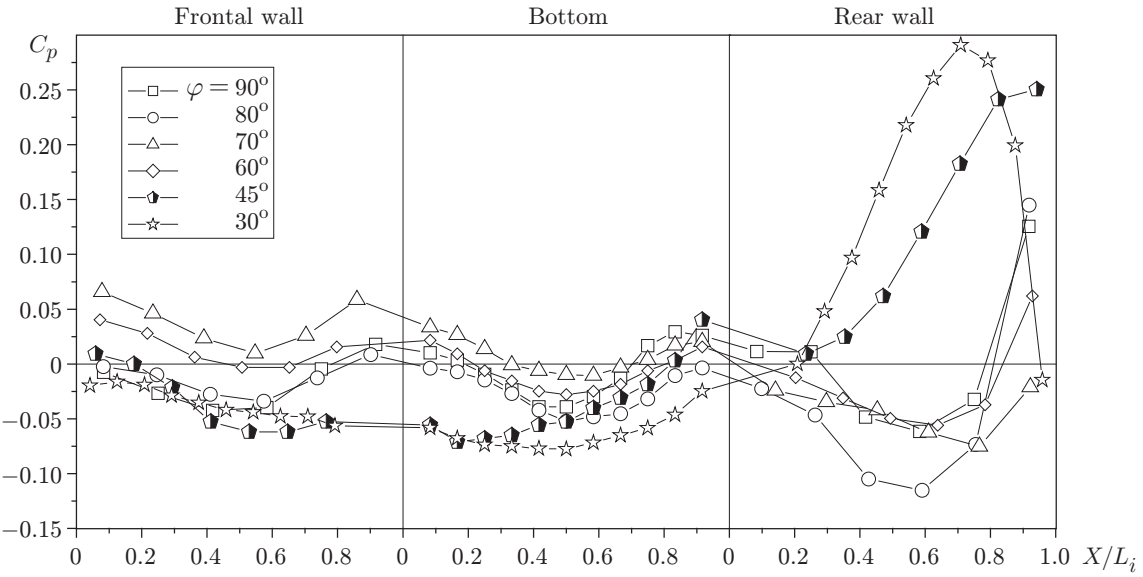


Fig. 6. Pressure distribution over the mid-section of the cavity.

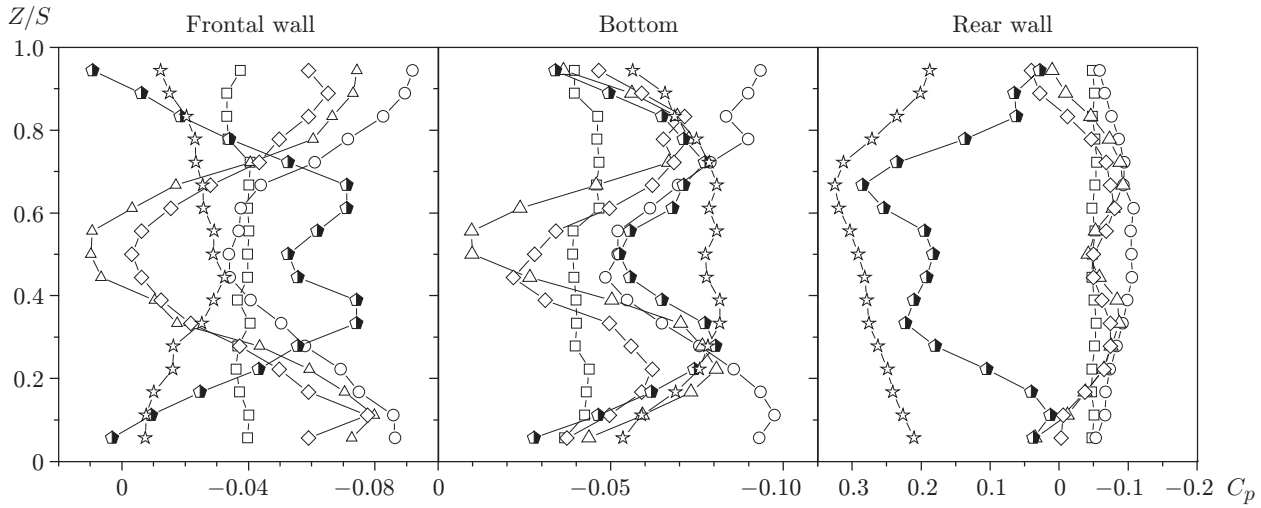


Fig. 7. Pressure distribution over the cavity span (notation the same as in Fig. 6).

coefficients were measured over the mid-section of the bottom surface and also on the frontal and rear walls. In addition, cross-sectional pressure distributions were measured in the center of the cavity bottom and on the frontal and rear walls at a distance of 40 mm from the cavity edges.

A typical distribution of the pressure coefficient along the cavity is plotted in Fig. 6. At $\varphi = 90$, 80, and 70°, the character of the curves in Fig. 6 is identical; the value of $C_p$ slightly increases with decreasing angle. The highest pressure is observed on the frontal wall; its values are lower on the bottom and on the rear wall, and rarefaction is observed on the cavity bottom. The pressure significantly increases toward the exit edge. At $\varphi = 60°$, when a two-cell flow structure is formed, the pressure starts decreasing. At $\varphi = 45$ and 30°, the character of the pressure distribution becomes essentially different: rarefaction on the frontal wall and on the cavity bottom and a significant increase in pressure on the rear wall. At $\varphi = 45°$, the coefficient $C_p$ at the exit edge is approximately twice its value at $\varphi = 90°$. At $\varphi = 30°$, the reattachment point is shifted to the cavity, and the pressure maximum is located near the exit edge.

Pressure redistribution caused by vortex formation is even more clearly observed in cross sections (Fig. 7). At $\varphi = 90°$, the pressure over the cavity span is almost uniform on both walls and on the cavity bottom. At $\varphi = 80°$

and especially at $\varphi = 70$ and 60°, suction of mass in the center of the cavity, directed opposite to the main flow, results in strong asymmetry of the distributions of pressure coefficients with a maximum in the mid-section and significant rarefaction near the butt-end faces and on the bottom. Formation of a two-cell vortex is most clearly seen in the pressure distribution at $\varphi = 45°$: there are two minimums in the center of the cells on the frontal wall and on the bottom, and the pressure drastically increases near the butt-end faces. The increase in pressure is especially noticeable on the rear wall, the centers of the cells corresponding to pressure maximums. At $\varphi = 30°$, the pressure distributions on all walls are more uniform. The increase in pressure on the rear wall is even greater than that at $\varphi = 45°$.

Thus, reconstruction of the cavity flow with decreasing angles of inclination of the frontal and rear walls leads to significant changes in the distribution of the pressure coefficients. The estimates show that the pressure coefficient averaged over the surface in a cavity with $\varphi = 30°$ is approximately 20% higher than that in a rectangular cavity. The flow evolution and the pressure distributions indirectly suggest that heat transfer may become more intense with decreasing angle $\varphi$.

**Conclusions.** Flow patterns in cavities with inclined walls have been visualized. The flow is shown to become unstable in the range of inclination angles $\varphi = 70$–60°. The primary vortex decomposes into two vortices. At low angles, the flow structure exerts a substantial effect on pressure coefficients.

This work was supported by the Russian Foundation for Basic Research (Grant No. 04-02-16070) and by the Foundation "Leading Scientific Schools of the Russian Federation" (Grant No. NSh-1308.2003.8).

## REFERENCES

1. D. J. Maull and L. F. East, "Three-dimensional flow in cavities," *J. Fluid Mech.*, **16**, No. 4, 620–632 (1963).
2. A. L. Kistler and F. C. Tan, "Some properties of turbulent separated flows," *Phys. Fluids Suppl.*, **10**, No. 9, 165–173 (1967).
3. R. I. Haugen and A. M. Dhanak, "Heat transfer in turbulent boundary-layer separation over a surface cavity," *Trans. ASME, J. Heat Transfer*, **89**, No. 4, 335–340 (1967).
4. D. Rockwell and E. Naudasher, "Review. Self-sustaining oscillations of flow past cavities," *Trans. ASME, J. Fluids Eng.*, **100**, 152–165 (1978).
5. A. D. Gosman, E. E. Khalil, and J. H. Whitelaw, "The calculation of two-dimensional turbulent recirculating flows," in: *Turbulent Shear Flows*, Vol. 1, Springer Verlag, Heidelberg (1979).
6. V. D. Zhak, V. A. Mukhin, and V. E. Nakoryakov, "Three-dimensional vortex structures in cavities," *J. Appl. Mech. Tech. Phys.*, **22**, No. 2, 186–189 (1981).
7. J. R. Koseff and R. L. Street, "On end wall effects of a lid driven cavity flow," *Trans. ASME, J. Fluids Eng.*, **106**, 385–389 (1984).
8. M. Hiwada, I. Mabuchi, and M. Kumada, "Three-dimensional flow and heat transfer in a rectangular cavity," *Heat Transfer Jap. Res.*, **14**, No. 1, 75–96 (1985).
9. I. M. Varfolomeev, G. A. Glebov, Yu. F. Gortyshov, et al., "Turbulent separation flow characteristics in a cavity," *J. Eng. Phys. Thermophys.*, **48**, No. 3, 387–391 (1985).
10. E. M. Sparrow and D. L. Misterek, "Mass transfer on the base of a cylindrical cavity in the floor of a flat duct," *Trans. ASME, J. Heat Transfer*, **108**, No. 4, 112–119 (1986).
11. K. Greichen and V. I. Kornilov, "Some features of a turbulent flow in a square cavity," Preprint No. 11-94, Inst. Theor. Appl. Mech., Sib. Div., Russian Acad. of Sci., Novosibirsk (1994).
12. A. A. Khalatov, G. V. Kovalenko, and S, G. Kobzar', "Modeling of hydrodynamics and heat transfer in an air flow past surfaces with cavities of different shapes," *Indust. Heat Eng.*, **26**, No. 5, 20–26 (2004).
13. V. I. Terekhov, N. I. Yarygina, and A. Yu. D'yachenko, "Turbulent heat transfer in a cross flow cavity with inclined sidewalls," in: *Proc. of the 12th Int. Heat Transfer Conf.* (Grenoble, France, August 18–23, 2002), Vol. 2, Elsevier, Paris (2002), pp. 615–619.
14. A. Yu. D'yachenko, V. I. Terekhov, and N. I. Yarygina, "Heat transfer in a crossflow cavity with inclined walls in a turbulized flow," in: *Proc. of the Vth Int. Forum on Heat and Mass Transfer* (Minsk, Belarus', May 24–28, 2004), Inst. Heat Mass Transfer, Minsk, CD ROM, No. 1-29.
15. V. Yu. Mityakov, "Capabilities of bismuth-based gradient heat-flux probes in a thermal engineering experiment," Candidate's Dissertation in Tech. Sci., St. Petersburg (2005).

16. H. Yamamoto, N. Seki, and S. Fukusako, "Forced convection heat transfer on heated bottom surface of a cavity," *Trans. ASME, J. Heat Transfer*, **101**, No. 3, 112–117 (1979),
17. F. R. Richards, M. F. Young, and J. C. Haiad, "Turbulent forced convection heat transfer from a bottom heated open surface cavity," *Int. J. Heat Mass Transfer*, **30**, No. 11, 2281–2287 (1987).
18. V. I. Terekhov and N. I. Yarygina, "Heat transfer in separation regions of turbulized flows," in: *Forced Convection of Single-Phase Fluid*, Proc. of the IInd Russian National Conf. on Heat Transfer (Moscow, October 26–30, 1999), Vol. 2, Moscow Energy Inst., Moscow (1998), pp. 244–247.
19. V. I. Terekhov, N. I. Yarygina, A. Yu. D'yachenko, and A. V. Shaporin, "Specific features of vortex formation and heat transfer in three-dimensional crossflow cavities," in: *Proc. IVth Int. Forum on Heat and Mass Transfer* (Minsk, Belarus', May 22–26, 2000), Vol. 1, Inst. Heat Mass Transfer, Minsk (2000), pp. 28–35.
20. H. C. Kuhlman, M. Wanschura, and H. J. Rath, "Elliptic instability in two-sided lid-driven cavity flow," *Europ. J. Mech., B: Fluids*, **17**, No. 4, 561–569 (1998).